Journal of Leather Science and Engineering

RESEARCH Open Access

An exploration of enhancing thermal stability of leather by hydrophilicity regulation: effect of hydrophilicity of phenolic syntan

Qingyong Sun[1,3], Yunhang Zeng[1], Yue Yu[1], Ya-nan Wang[1,2*] and Bi Shi[1,2]

Abstract

Effect of retanning on the thermal stability of leather is eliciting increasing attention. However, the relationship between the hydrophilicity of retanning agents and the heat resistance of leather and the corresponding mechanism remain unclear. Herein, phenolic formaldehyde syntans (PFSs) were selected as models to explore the effect of the hydrophilicity of retanning agents on the thermal stability of retanned leather. The thermal stability of leather was closely correlated to the hydrophilic group content (sulfonation degree) of PFSs. As the sulfonation degree increased, the water absorption rate of PFSs and their retanned leathers decreased, whereas the thermal stability of leather increased. Molecular dynamics simulation results proved that the introduction of PFSs could reduce the binding ability of collagen molecules with water and thus decreased the water molecules around the PFS-treated collagen. These results may provide guidance for the tanners to select retanning agents reasonably to improve the thermal stability of leather.

Keywords: Thermal stability, Phenolic formaldehyde syntan, Hydrophobicity, Water content, Molecular dynamics simulation

*Correspondence: wangyanan@scu.edu.cn

[1] National Engineering Laboratory for Clean Technology of Leather Manufacture, Sichuan University, Chengdu 610065, China
Full list of author information is available at the end of the article

Graphical Abstract

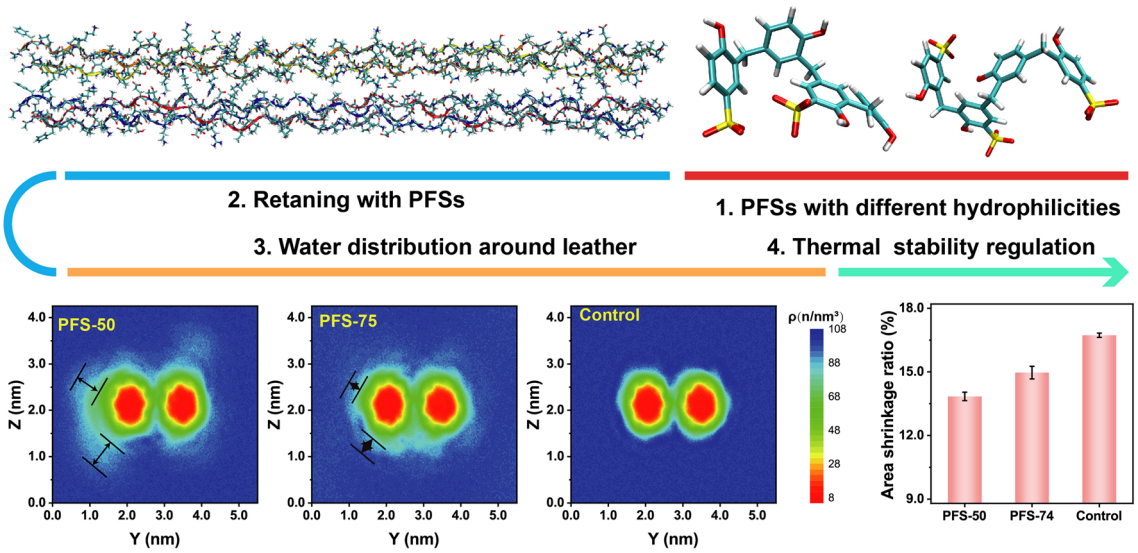

1 Introduction

Crust leathers obtained from post-tanning (mainly retanning, dyeing and fatliquoring) are not ultimate leather products, which will undergo further thermal treatments in subsequent processing inevitably. For example, ironing and embossing treatments in the finishing process are required to produce leather with smooth or different grain patterns. Certain shoe shapes need thermal setting and vulcanizing during footwear manufacturing [1]. In addition, long-time exposure to sunlight is inevitable in the course of using, especially for automotive leather. During these thermal treatments, not only tanning, but retanning contributes to the thermal stability of resultant leather. Therefore, understanding the mechanism of retanning agents on the thermal stability of crust leather is crucial for designing new leather chemicals to improve its usability.

The properties of leather/collagen, such as thermal stability and physical properties, are closely correlated with their water content [2, 3]. Schroepfer investigated the thermal stability of untanned and tanned bovine collagen with different hydration degrees by using differential scanning calorimetry (DSC) and confirmed that crosslinking degrees and drying increased the denaturation temperature of bovine hide collagen [4]. Komanowsky found no significant difference in the thermal denaturation temperature between raw and tanned leather when the moisture content was lower than 30% [5]. Tang investigated the dry heat resistance of hide and leather by using hot stage microscopy and found that the drying process was beneficial to increase the dry heat stability of hide powder [6]. Therefore, water content in leather may be an important factor that affects the thermal ability of tanned leathers. However, only a few research addresses the effect of retanning process on the thermal stability of leather. Generally, the thermal stability of retanned leather is evaluated by measuring the area loss of conditioned leathers at a certain temperature for some time according to ISO 17227. Wu [7] evaluated the effect of commonly used retanning agents in the leather industry on the dry heat resistance of leather by using this method. The dry heat resistance of leather treated by different types of retanning agents was in the order of phenolic formaldehyde syntan (PFS), acrylic resin, amino resin, quebracho extract, and chromium tanning agent. Further fourier transform infrared spectroscopy (FTIR) and thermogravimetry (TG) analysis revealed that the dry heat resistance may be correlated to the hydrophilicity of retanning agents. However, the structure of retanning agents is quite different and complex. The reason PFS has the best dry heat resistance and the effect of the hydrophilicity of retanning agent on the dry heat resistance of leather still need to be further investigated.

PFSs are generally prepared through condensation, and sulfonation by using phenol, formaldehyde, and concentrated sulfuric acid as raw materials, thereby containing hydrophobic benzene rings and hydrophilic sulfonic acid groups, which are typically amphiphilic compounds [8, 9]. Therefore, regulating the water content and corresponding thermal stability of leather by

adjusting the hydrophilicity of PFS through sulfonation is possible.

In this study, PFSs with sulfonation degree (DS) of 50%, 63%, and 74% were selected to explore the effect of hydrophilicity on the thermal stability of leather. The dispersion of collagen fiber of PFS retanned leather and the thermal stability of retanned leather were compared. In addition, molecular dynamic (MD) simulations were performed to investigate the changes in water distribution surrounding the collagen for leathers treated by PFSs with different DSs. As a result, the relationship between the hydrophilicity of PFSs and the thermal stability of leathers were analyzed. This work is expected to provide theoretical guidance to leather chemical companies in designing new products and tanners in selecting suitable chemicals for the production of high-thermal-stability leathers, especially chrome-free leathers.

2 Experimental

2.1 Materials

Chrome tanned cattle hide with a thickness of 1.2 mm and Cr_2O_3 content of 4.5% was purchased from a local tannery in China. PFSs named PFS-50, PFS-63, and PFS-74 with DS of 50%, 63% and 74% were prepared according to our previous work [10]. The prepared PFSs have a polymerization degree of 3–7 and a molecular weight of about 500 g/mol [10]. Chemicals used for leather processing were of commercial grade and were provided by the Sichuan Decision New Material Technology Co., Ltd. (China).

2.2 Water adsorption behavior of PFSs

The lyophilized PFSs were first dried to constant weight at 105 ± 2 °C in an oven. Subsequently, the water absorption experiments were conducted at a temperature of 20 ± 2 °C and relative humidity of 65 ± 5% for 48 h. The water absorption rates with time were recorded.

2.3 Retanning experiments

Four pieces of shaved wet blue (30 cm × 30 cm for each), which were cut symmetrically from the back region of the cattle hide, were rewetted and neutralized to pH 6.5. Then, they were retanned with PFSs according to the process in Table 1, and the crust leather without PFS retanning was used as the control. After retanning for 120 min, leather samples were taken for moisture absorption and thermogravimetric analysis to explore the relationship between the thermal stability of leather and hydrophilicity of PFSs. The remaining leather samples were fatliquored, dried, staked and air-conditioned for 48 h (20 ± 2 °C, RH 65 ± 5%). Subsequently, the thickness, tear strength and tensile strength of crust leathers were measured according to IUP 4, IUP 6 and IUP 8, respectively. The water content, area loss, the shrinkage temperature, and porosity of the crust leathers before and after dry heat resistance test were measured.

2.4 Analysis of leather

2.4.1 Moisture absorption behavior

The dried leather samples were firstly grounded into leather fibers with a diameter of approximately 2 mm using a cutting mill (SM 100, Retsch, Germany). Then, about 0.5 g of leather fibers were dried to a constant weight (w_0) at 105 °C ± 2 °C. Next, they were reconditioned (20 °C ± 2 °C, RH 65% ± 5%) for 48 h, and the weight of the test samples at time t (h) during the conditioning was recorded as w_t, and the moisture absorption rate q_t at time t was calculated as Eq. (1).

$$q_t = \frac{w_t - w_0}{w_0} \times 100\% \quad (1)$$

2.4.2 Water content

The water content of the crust leathers was determined in accordance to the standard test method ISO 4684 after they were conditioned for 48 h (20 °C ± 2 °C, RH 65% ± 5%).

Table 1 Retanning and fatliquoring processes

Process	Chemicals	Dosage[a] (%)	Temperature (°C)	Time (min)	Remark
Retanning	Water	200	35	120	
	PFS[b]	15			Collect leather samples
Fatliquoring	Synthetic fatliquor	8.0		60	
	Formic acid	0.5 × n		15 × n	pH 3.8, drain
Washing	water	200		10	
Vacuum drying at 50 °C for 3 min, hang-drying and staking					Collect crust leather samples

[a] The percentage of chemicals was based on the weight of the shaved wet blue

[b] The PFS used were PFS-50, PFS-63, and PFS-74

2.4.3 Dry heat resistance

The dry heat resistance of crust leathers was evaluated by determining the area loss according to the standard test method ISO 17227 at 150 °C ± 5 °C for 30 min ± 0.5 min. The lower the area loss is, the better the dry heat resistance of retanned leather will be.

2.4.4 TG analysis

Thermal weight loss of the retanned leather samples after air conditioning were determined by a thermogravimetric analyzer (TG209F1, Netzsch, Germany) from 35 °C to 700 °C at a heating rate of 10 K/min under a nitrogen atmosphere.

2.4.5 Shrinkage temperature

The crust leathers before and after dry heat resistance test were fully rewetted in water, and then their shrinkage temperature (Ts) was measured using a digital leather shrinkage temperature instrument (MSW-YD4, Shaanxi University of Science and Technology, China). Ts difference before and after dry heat resistance test was recorded as ΔTs.

2.4.6 Porosity

The porosity of the crust leather before and after dry heat resistance test was measured using a mercury intrusion porosimeter (AutoPore IV 9500, Micromeritics, USA) according to the literature [11]. The test samples were cut from the flat part of the crust leathers, and the dimension of the test samples was 3 cm × 2 cm (approximately 0.6 g). The pressure was set as 33 000 psia, and the equilibration time was set as 10 s.

2.5 MD simulation

MD simulation was performed to investigate the effect of DS of PFSs on the collagen–water interaction.

The collagen molecule model (COL) with an initial triplet helix was constructed by the TheBuScr (Triple Helical collagen Building Script) code [12] and PyMOL software [13]. The sequences (Table 2) were selected from the real bovine type I collagen (Swiss Protein bank, entry number P02453 for α_1 chain and entry number P02465 for α_2 chain) [14]. The amino acid composition (by %) of the selected sequences is similar to the composition of the complete collagen molecule, and the six residues of the two ends are the same for α_1 and α_2 chains, thereby avoiding the possible boundary effects [15]. The N-terminal and C-terminal for each chain were caped with acetyl group and *N*-methylamine group, respectively, to eliminate artifacts induced by charges at both ends [16]. Notably, hydroxyproline (Hyp) is a nonstandard residue, the (***P***) in the Y position of the repeated Glycine-X–Y triplet in the sequences stands for Hyp. The structure of the

Table 2 Sequence of the collagen peptide used for constructing collagen model

α_1	GF***P***GPKGAAGE***P***GKAGERGV***P***GP***P***GAVGPAGKDGEAGAQGP***P***GPAGPAGERGEQGPA
α_2	GF***P***GPKGPSGD***P***GKAGEKGHAGLAGARGA***P***GPDGNNGAQGP***P***GLQGVQGGKGEQGPA
α_1'	GF***P***GPKGAAGE***P***GKAGERGV***P***GP***P***GAVGPAGKDGEAGAQGP***P***GPAGPAGERGEQGPA

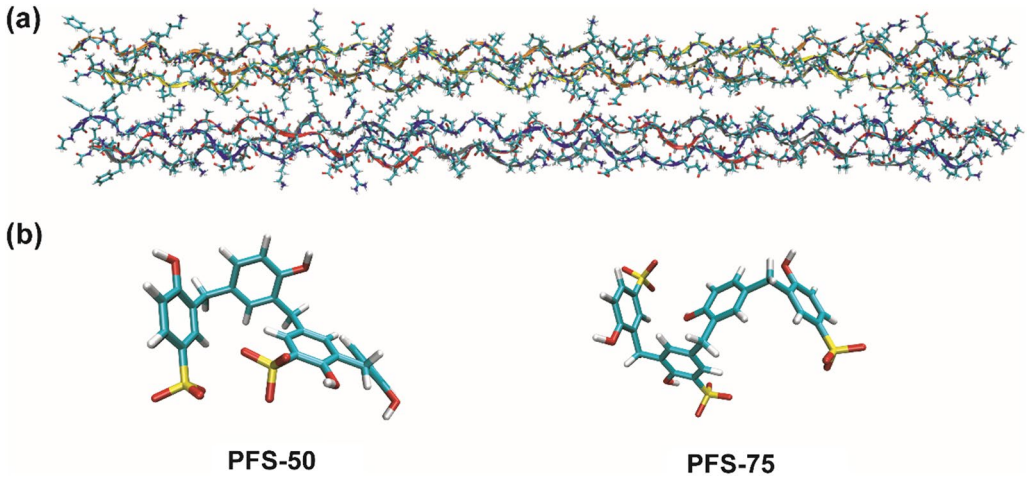

Fig. 1 Structure of **a** COL and **b** PFS-50 and PFS-75

constructed bi-molecular collagen model is illustrated in Fig. 1a.

Two analogs (Fig. 1b) generated by PyMOL software were selected as models. PFS-50 consists of four phenol units and two sulfonic acid units (DS = 50%), and PFS-75 consists of four phenol units and three sulfonic acid units (DS = 75%). Before MD simulation, the initial structures of PFS-50 and PFS-75 were optimized through density functional theory by using the B3LYP function at the 6-311G++ (d, p) basis set.

MD simulations were carried out by using the GROMACS package [17] (version 2020.6). The CHARMM36 force fields [18] and the CHARMM General Force Field (CGenFF) were used to describe the COL and the PFSs molecule respectively [19]. Meanwhile, the modified TIP3P water model was used to describe the water molecules [20]. The simulation details of System 1 to 3 are shown in Table 3. The configuration of the three systems was generated by the built-in modules of GROMACS. Na^+ ions were added to neutralize the negative charges of the three systems. Periodic boundary conditions were applied to the x, y, and z directions.

The MD simulation procedures are detailed as follows: (1) All systems were energy minimized by using the steepest-descent minimization method for 10,000 steps until the maximum force becomes less than 100 $kJ{\cdot}mol^{-1}{\cdot}nm^{-1}$. (2) The energy minimized systems were heated from 0 to 300 K within 100 ps and equilibration for another 400 ps under the NVT canonical ensemble (number of substance [N], volume [V], and temperature [T] were conserved), followed by a 500 ps of NPT equilibration (number of substance [N], pressure [P] and temperature [T] were conserved) at 300 K and 1 atm. (3) After that, all systems were subjected to production runs for another 30 ns. The integration time step was set to 2 fs. The non-bond interactions (e.g., van der Waals and short-range electrostatic interaction) cut-off were set to 1.2 nm. V-rescale thermostat [21] and Parrinello–Rahman barostat [22] were used to control the temperature and pressure. The LINCS algorithm [23] was applied to constrain the bond length of hydrogen atoms. The PME algorithm [24] was applied to treat the long-range electrostatic interactions. Visualization and analysis of the simulation trajectories were carried out by using the VMD software [25] and built-in modules of GROMACS.

3 Results and discussion

3.1 Effect of DS on the water adsorption behavior of PFSs

PFSs were prepared from phenolic formaldehyde condensates through sulfonation reaction by using different amounts of concentrated sulfuric acid (Fig. 2a). Thus, the prepared PFSs have a DS gradient. Figure 2b shows that the water absorption rate of PFSs was highly

Table 3 Simulation details

System	Composition	Number of COL	Number of PFS	Number of water molecule	Volume of box
System 1	COL–PFS-50–Water	1	25	13,500	19.0 nm × 5.6 nm × 4.3 nm
System 2	COL–PFS-75–Water	1	25	13,500	19.0 nm × 5.6 nm × 4.3 nm
System 3	COL–Water	1	0	13,500	19.0 nm × 5.6 nm × 4.3 nm

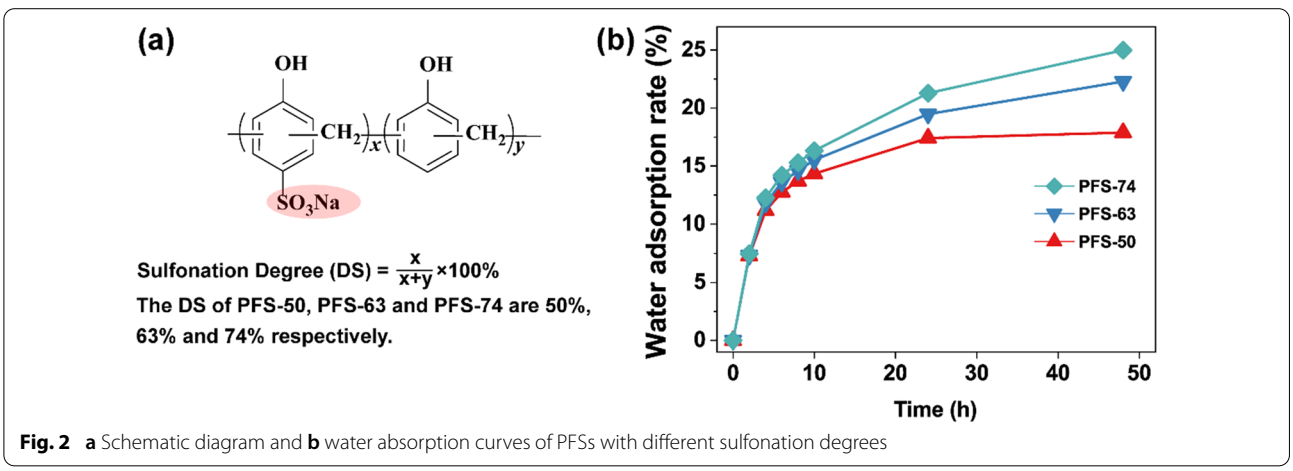

Fig. 2 **a** Schematic diagram and **b** water absorption curves of PFSs with different sulfonation degrees

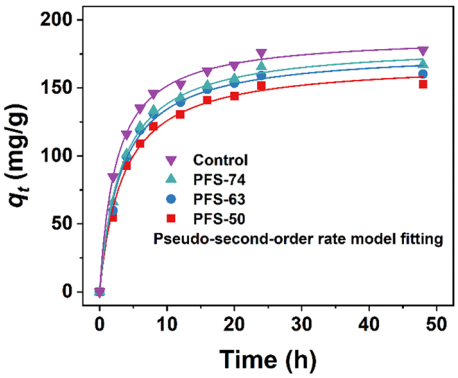

Fig. 3 Water absorption curve of PFSs retanned leathers and control leather (pseudo-second-order rate model fitting)

Table 4 Adsorption kinetics parameters fitted by the pseudo-second-order rate model

No.	Pseudo-second-order rate model		
	k_2	$q_{e\,cal}$	R^2
PFS-50	0.0017	169.5	0.995
PFS-63	0.0017	177.6	0.994
PFS-74	0.0017	182.6	0.997
Control	0.0022	188.5	0.998

DS-dependent. The water adsorption rate increased from 17.9% to 25.0% as DS of PFSs increased from 50% to 74%. This result can be explained by the fact that the increased sulfonic acid groups are prone to forming a hydrogen bond with water [10], and therefore the PFSs with higher DS absorb more water.

3.2 Effect of DS on the water adsorption of PFSs retanned leather

To evaluate the hydrophilicity of PFS retanned leathers, the grounded leather samples were first dried to constant weight, and then the water adsorption rate of PFSs retanned leather with time was determined under standard air conditions. Figure 3 shows that the water adsorption rate of retanned leathers increased sharply during 0–9 h and then gradually reached equilibrium within approximately 24 h. To further investigate the adsorption behavior and binding mode of PFSs retanned leather with water, the pseudo-second-order rate model (Eq. 2) was used to fit the obtained adsorption rate data.

$$t/q_t = 1/k_2 q_e^2 + t/q_e, \tag{2}$$

where k_2 [mg/ (g·h)] is the pseudo-second-order rate constant, q_e and q_t are the adsorption capacity (mg/g) of water at equilibrium and at time t (h). The calculated parameters of the pseudo-second-order rate model are given in Table 4. The correlation coefficient (R^2) for all of the four retanned leather were consistently higher than 0.99, indicating that the adsorption of water to the retanned leathers was chemisorption controlled [26]. The water molecules adsorbed on the leather might bind with the carboxyl, amino, and hydroxyl groups of collagen by means of hydrogen bonds. The lower rate constant (k_2) in the PFS retanned leather compared with that in the control group indicated that the PFSs retanned leathers had a lower adsorption rate to water than the control leather. This result suggested that the hydrophilicity of the collagen was decreased as PFS was introduced to leather. In addition, the adsorption capacity of water increased with DS, which was consistent with the results in Fig. 2b.

To further explore the effect of DS on the water absorption behavior of retanned leather, the distribution and number density change of water molecules that surround the collagen molecule before and after PFS retanning were simulated and analyzed. As illustrated in Fig. 4a, the total number of water molecules in each system was the same (13,500), but the number density of water molecules in the YZ plane from 10 to 30 ns (the system reached equilibrium at 10 ns) of System 1 to 3 were different. PFS-50-COL-water system had a more low-density region (light blue) of water around COL, followed by the PFS-75-COL-Water system, and the COL-Water system without PFSs had the least such region. Generally, the H-bond is considered to be formed when the distance between hydrogen acceptor (O, N) and hydrogen donor (O–H, N–H) < 3.5 Å and the angle of hydrogen–donor–acceptor < 30° [27, 28]. Therefore, the number of water molecules bonded through H-bond with collagen molecule around COL within 3.5 Å (Fig. 4b) and their distribution (Fig. 4c) from 10 to 30 ns were calculated and analyzed for all three systems. The water number within 3.5 Å of COL showed the order of PFS-50 < PFS-75 < Control. These results suggested that the introduction of PFSs would weaken the binding of collagen with water and increase the hydrophobicity of the treated collagen. Moreover, the lower the DS of PFSs is, the stronger the hydrophobicity of the treated COL will be. These results were consistent with the water absorption rate of retanned leather (Fig. 3). Therefore, controlling the hydrophilicity of PFSs by adjusting their DS can regulate the water binding ability of retanned leather.

3.3 Effect of DS on the thermal stability of PFSs retanned leathers

The physical properties, such as tear strength and tensile strength of leathers retanned by different PFSs did not show any obvious differences (Additional file 1:

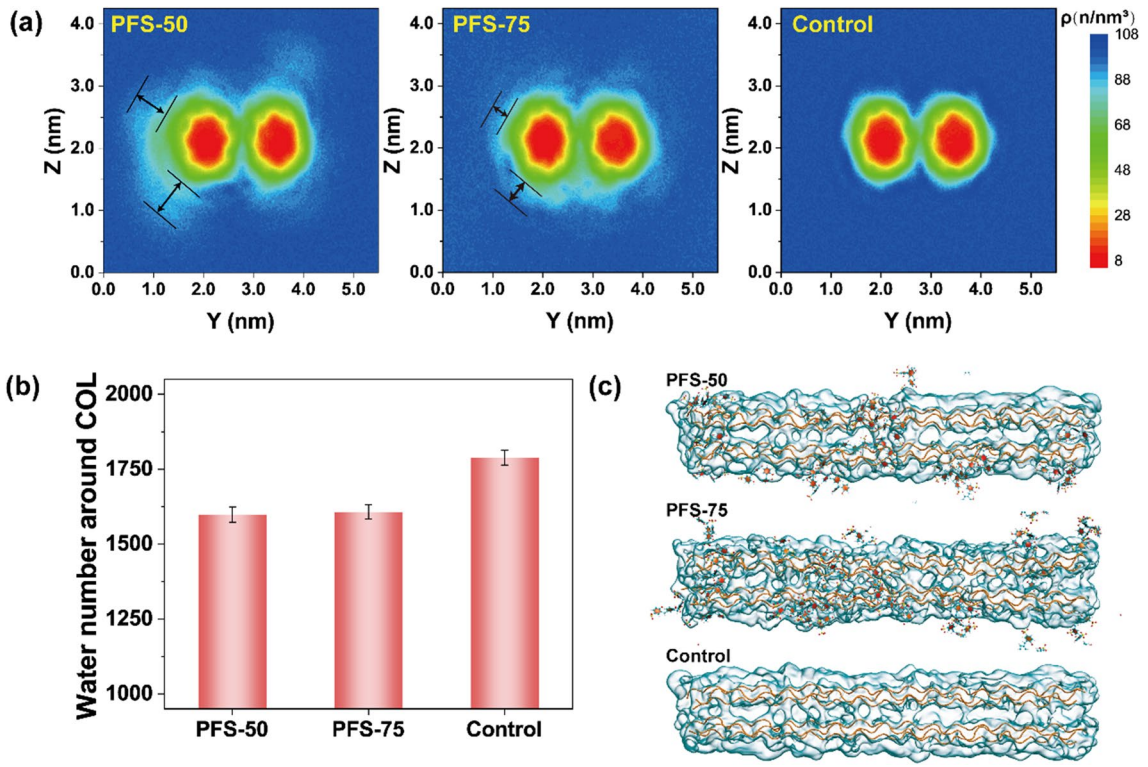

Fig. 4 **a** Average number density of water molecules around COL from 10 to 30 ns; **b** average number of water molecules within 3.5 Å of COL from 10 to 30 ns; **c** distribution of water molecules within 3.5 Å of COL

Table S1). As mentioned above, PFSs with different DSs can impart the retanned leather with different water adsorption abilities, which will affect the water content of the crust leather inevitably. Therefore, the water content of the conditioned crust leathers was measured prior to the dry heat resistance tests. As shown in Fig. 5a, the water content of PFS retanned leathers was less than those of control leather and increased with DS. This result was consistent with the water adsorption result of the retanned leathers (Fig. 3). Considering the fact that the fatliquoring and drying processes were the same, the water content increase of the crust leather should be mainly due to the decrease in DS of PFS.

The area loss of PFS retannned leather was less than that of control leather and increased with the increase in DS (Fig. 5b). The dry heat resistance of leather seemed to be negatively correlated with the water content of leather. This finding indicated that the dry heat

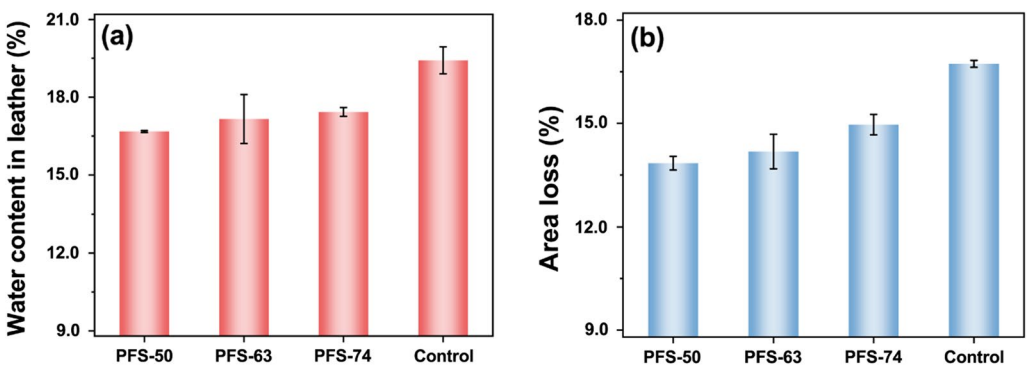

Fig. 5 Water content **a** and area loss **b** of leathers retanned by using PFS with different sulfonation degree and control leather

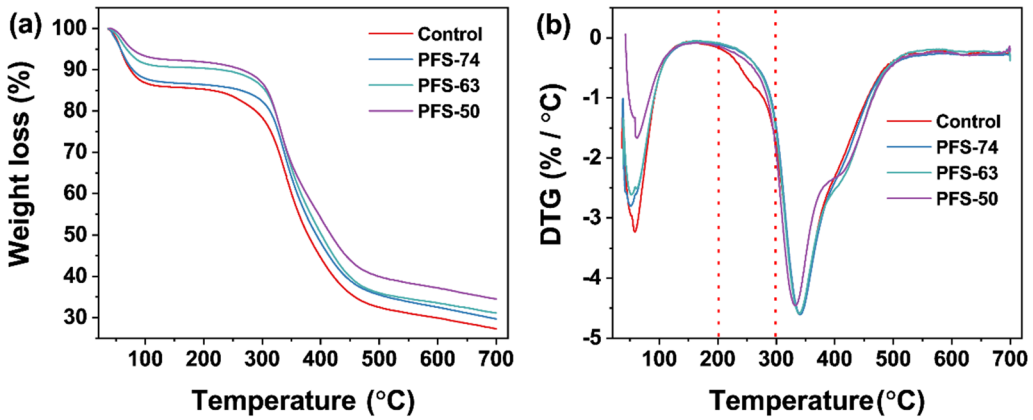

Fig. 6 **a** Weight loss and **b** differential thermogravimetry (DTG) curves of PFSs retanned and control leathers

Table 5 Weight loss of PFSs retanned leathers and control leather at different stages and residual weight

Leather sample	Weight loss (%) at 40–150 °C	Weight loss (%) at 200–500 °C	Residual weight (%)
PFS-50 retanned leather	7.7	52.0	34.5
PFS-63 retanned leather	9.4	54.4	31.1
PFS-74 retanned leather	13.2	50.9	29.7
Control leather	14.2	52.8	27.3

resistance of retanned leather can be regulated by adjusting the combination ability of leather and water through the DS of PFS. However, the tanning power of PFSs will also be an important factor that affects the dry heat resistance of PFSs retannned leather.

The thermal weight loss of retanned leathers was analyzed further. As shown in Fig. 6, two distinct thermal weight-loss stages during the heating of the retanned leather were observed. The first one (40 °C to 150 °C) was mainly related to the water loss [29]. The weight loss ratio (Table 5) in this stage was consistent with the water adsorption capacity (q_e) of retanned leather (Table 4). Considering that the moisture content in leather is an important factor in maintaining the distance of collagen fiber [30–34], the loss of water was prone to decreasing the distance between collagen fibers, and higher water loss caused greater changes in fiber distance and area loss (Fig. 5b). The second weight-loss stage (200 °C to 500 °C) was associated with the thermal decomposition of the collagen chain [35]. The residual weight at 700 °C (Table 5) showed the order of PFS-50 retanned leather > PFS-63 retanned leather > PFS-74 retanned leather > control leather, that is, the lower the DS of PFS is, the higher amount of organic matter that was not removed in the nitrogen atmosphere will be.

The Ts that reflects the hydrothermal stability of the retanned leather before and after dry heat resistance test is shown in Fig. 7a. Slight difference was observed in the Ts of crust leathers before dry heat resistance tests. This phenomenon is mainly due to the fact that the chrome

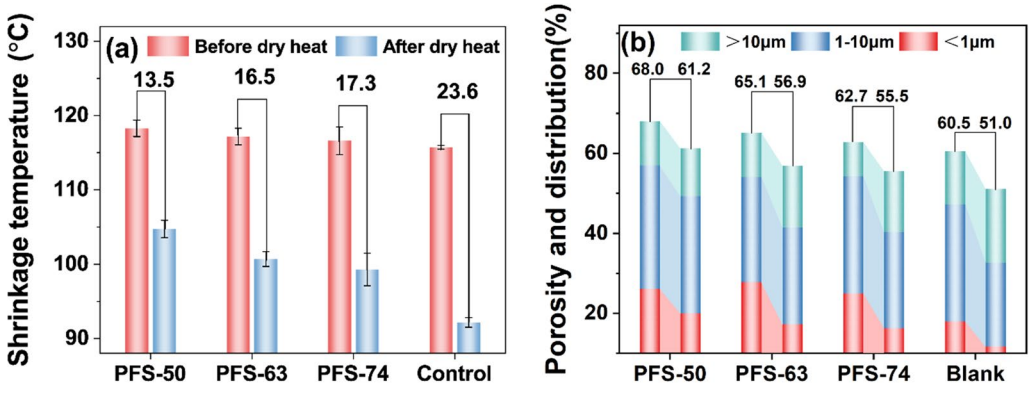

Fig. 7 The **a** shrinkage temperature and **b** porosity of retanned leathers before and after dry heat resistance test

tanned leather is highly stabilized [36], and the tanning effect that PFSs played is limited. After dry heat resistance test, the Ts of all of the retanned leathers decreased because the supramolecular collagen matrix of leather may be damaged to some extent during dry heating test at 150 °C. The ΔTs showed the order of PFS-50 retanned leather < PFS-63 retanned leather < PFS-74 retanned leather < control leather. Collagen is surrounded by a supramolecular water sheath nucleated at the hydroxyproline side chains [37]. When PFS with lower DS was introduced into collagen, it can replace more water molecules around collagen than the PFS with higher DS (Fig. 4). This will cause the fibers to approach more closely and increase the stability of retanned leather [36, 38].

As previously mentioned, PFS with low DS increased hydrophobicity and thereby decreased water content in the resulted leather. This instance may enhance the dispersion of the collagen fiber of PFSs retanned leather [39]. The experimental results shown in Fig. 7b validate our speculation. The porosity of retanned leather increased with the decrease in DS of PFS. After dry heat resistance test, the porosity, particularly the proportion of small pores ($\Phi < 1$ μm), of all the retanned leather decreased because of water loss and thermal denaturation. However, the porosity of PFS-50 retanned leather had a higher porosity compared with the others because it was more thermally stable. Thus the porosity structure of the retanned leather can be maintained well.

4 Conclusion

The thermal stability of leather is closely associated with the DS of PFSs. Reducing the DS of PFSs can reduce the affinity of leather to water and the corresponding water content in leather, thereby reducing the area loss of leather under high temperature. PFSs with a low DS can also reduce the denaturation of leather so that a higher porosity of leather can be maintained after dry heat resistance test. As such, the thermal stability of retanned leathers can be regulated by adjusting the hydrophobicity of the retanning agents used.

Abbreviations

PFS: Phenolic formaldehyde syntan; MD: Molecular dynamic; DS: Sulfonation degree; TG: Thermogravimetry; DSC: Differential scanning calorimetry; Ts: Shrinkage temperature.

Supplementary Information

The online version contains supplementary material available at https://doi.org/10.1186/s42825-022-00096-1.

Additional file 1. Table S1. Physical properties of leathers.

Acknowledgements

We thank Prof. Wenhua Zhang from National Engineering Laboratory for Clean Technology of Leather Manufacture, Sichuan University for guiding molecular dynamic calculations. We also thank Dr. Jinwei Zhang from National Engineering Laboratory for Clean Technology of Leather Manufacture, Sichuan University for his support for leather processing.

Author contributions

QS, YW and BS conceived the idea. QS performed the experiments and drafted the manuscript. YY participated in part of the experiments. YZ analyzed the results. YW and BS revised the manuscript. All authors read and approved the final manuscript.

Funding

This work was supported by the National Natural Science Foundation of China (21978176).

Availability of data and materials

All data from this study are presented in the paper.

Declarations

Competing interests

The authors declare that they have no competing interests.

Author details

[1]National Engineering Laboratory for Clean Technology of Leather Manufacture, Sichuan University, Chengdu 610065, China. [2]Key Laboratory of Leather Chemistry and Engineering (Sichuan University), Ministry of Education, Chengdu 610065, China. [3]Sichuan Decision New Material Technology Co., Ltd., Deyang 618000, China.

Received: 14 June 2022 Revised: 12 July 2022 Accepted: 25 July 2022
Published online: 15 August 2022

References

1. Miller RG, Department CT. Manual of shoemaking. Clarks; 1989.
2. Huang Y, Xiao H, Pu H, Xue N, Hao B, Huang X, et al. Self-driven directional dehydration enabled eco-friendly manufacture of chrome-free leather. J Leather Sci Eng. 2022;4(1):17. https://doi.org/10.1186/s42825-022-00089-0.
3. Amanov A, Khurramov SR, Bahadirov GA, Abdukarimov A, Amanov TY. Modeling of strain and filtration properties of a semi-finished leather product. J Leather Sci Eng. 2021;3(1):14. https://doi.org/10.1186/s42825-021-00056-1.
4. Schroepfer M, Meyer M. Dsc investigation of bovine hide collagen at varying degrees of crosslinking and humidities. Int J Biol Macromol. 2017;103:120–8. https://doi.org/10.1016/j.ijbiomac.2017.04.124.
5. Komanowsky M. Thermal-stability of hide and leather at different moisture contents. J Am Leather Chem Assoc. 1991;86(8):269–80.
6. Tang KY, Liu J, Wang F, Cao J. Dry heat resistance of hide and leather. J Am Leather Chem Assoc. 2003;98(5):168–72.
7. Wu C, Zeng YH, Liao XP, Zhang WH, Shi B. Effect of retanning agents on dry heat resistance of leathers. J Am Leather Chem Assoc. 2013;108(8):294–9.
8. Chen L, Dou J, Ma Q, Li N, Wu R, Bian H, et al. Rapid and near-complete dissolution of wood lignin at ≤ 80 °C c by a recyclable acid hydrotrope. Sci Adv. 2017;3(9): e1701735. https://doi.org/10.1126/sciadv.1701735.
9. Smith MD, Mostofian B, Cheng X, Petridis L, Cai CM, Wyman CE, et al. Cosolvent pretreatment in cellulosic biofuel production: effect of tetrahydrofuran-water on lignin structure and dynamics. Green Chem. 2016;18(5):1268–77. https://doi.org/10.1039/c5gc01952d.
10. Sun Q, Zeng Y, Wang Y-N, Yu Y, Shi B. A deeper exploration of the relation between sulfonation degree and retanning performance of aromatic syntans. J Leather Sci Eng. 2021;3(1):1–10. https://doi.org/10.1186/s42825-021-00073-0.

11. He X, Wang YN, Zhou JF, Wang HB, Ding W, Shi B. Suitability of pore measurement methods for characterizing the hierarchical pore structure of leather. J Am Leather Chem Assoc. 2019;114(2):41–7.
12. Rainey JK, Goh MC. An interactive triple-helical collagen builder. Bioinformatics. 2004;20(15):2458–9. https://doi.org/10.1093/bioinformatics/bth247.
13. DeLano WL. Pymol: an open-source molecular graphics tool. CCP4 Newsl Protein Crystallogr. 2002;40(1):82–92.
14. Brown EM. Development and utilization of a bovine type I collagen microfibril model. Int J Biol Macromol. 2013;53:20–5. https://doi.org/10.1016/j.ijbiomac.2012.10.029.
15. Chang SW, Shefelbine SJ, Buehler MJ. Structural and mechanical differences between collagen homo- and heterotrimers: relevance for the molecular origin of brittle bone disease. Biophys J. 2012;102(3):640–8. https://doi.org/10.1016/j.bpj.2011.11.3999.
16. Tang M, Gandhi NS, Burrage K, Gu Y. Adsorption of collagen-like peptides onto gold nanosurfaces. Langmuir. 2019;35(13):4435–44. https://doi.org/10.1021/acs.langmuir.8b03680.
17. Hess B, Kutzner C, van der Spoel D, Lindahl E. GROMACS 4: algorithms for highly efficient, load-balanced, and scalable molecular simulation. J Chem Theory Comput. 2008;4(3):435–47. https://doi.org/10.1021/ct700301q.
18. Croitoru A, Park SJ, Kumar A, Lee J, Im W, MacKerell AD Jr, et al. Additive CHARMM36 force field for nonstandard amino acids. J Chem Theory Comput. 2021;17(6):3554–70. https://doi.org/10.1021/acs.jctc.1c00254.
19. Vanommeslaeghe K, Hatcher E, Acharya C, Kundu S, Zhong S, Shim J, et al. CHARMM general force field: a force field for drug-like molecules compatible with the CHARMM all-atom additive biological force fields. J Comput Chem. 2010;31(4):671–90. https://doi.org/10.1002/jcc.21367.
20. Jorgensen WL, Chandrasekhar J, Madura JD, Impey RW, Klein ML. Comparison of simple potential functions for simulating liquid water. J Chem Phys. 1983;79(2):926–35. https://doi.org/10.1063/1.445869.
21. Bussi G, Donadio D, Parrinello M. Canonical sampling through velocity rescaling. J Chem Phys. 2007;126(1): 014101. https://doi.org/10.1063/1.2408420.
22. Parrinello M, Rahman A. Crystal structure and pair potentials: a molecular-dynamics study. Phys Rev Lett. 1980;45(14):1196–9. https://doi.org/10.1103/PhysRevLett.45.1196.
23. Hess B, Bekker H, Berendsen HJC, Fraaije JGEM. LINCS: a linear constraint solver for molecular simulations. J Comput Chem. 1997;18(12):1463–72.
24. Grimme S, Antony J, Ehrlich S, Krieg H. A consistent and accurate ab initio parametrization of density functional dispersion correction (DFT-D) for the 94 elements H-Pu. J Chem Phys. 2010;132(15): 154104. https://doi.org/10.1063/1.3382344.
25. Humphrey W, Dalke A, Schulten K. Vmd: Visual molecular dynamics. J Mol Graph. 1996;14(1):33–8. https://doi.org/10.1016/0263-7855(96)00018-5.
26. Tang KY, Zheng XJ, Yang M, Liu J, Shelly DC, Casadonte DJ. Influence of retanning on the adsorption capacity of water on cattlehide collagen fibers. J Am Leather Chem Assoc. 2009;104(11):367–74.
27. Luzar A, Chandler D. Hydrogen-bond kinetics in liquid water. Nature. 1996;379(6560):55–7. https://doi.org/10.1038/379055a0.
28. Jana B, Pal S, Bagchi B. Hydrogen bond breaking mechanism and water reorientational dynamics in the hydration layer of lysozyme. J Phys Chem B. 2008;112(30):9112–7. https://doi.org/10.1021/jp800998w.
29. Pietrucha K. Changes in denaturation and rheological properties of collagen-hyaluronic acid scaffolds as a result of temperature dependencies. Int J Biol Macromol. 2005;36(5):299–304. https://doi.org/10.1016/j.ijbiomac.2005.07.004.
30. Fullerton GD, Amurao MR. Evidence that collagen and tendon have monolayer water coverage in the native state. Cell Biol Int. 2006;30(1):56–65. https://doi.org/10.1016/j.cellbi.2005.09.008.
31. Malcolm A, Rougvie MA, Bear RS. An X-Ray Diffraction investigation of swelling by collagen. J Am Leather Chem Assoc. 1953;48:16.
32. Katz EP, Li ST. The intermolecular space of reconstituted collagen fibrils. J Mol Biol. 1973;73(3):351–69. https://doi.org/10.1016/0022-2836(73)90347-1.
33. Nomura S, Hiltner A, Lando JB, Baer E. Interaction of water with native collagen. Biopolymers. 1977;16(2):231–46. https://doi.org/10.1002/bip.1977.360160202.
34. Sasaki N, Shiwa S, Yagihara S, Hikichi K. X-ray diffraction studies on the structure of hydrated collagen. Biopolymers. 1983;22(12):2539–47. https://doi.org/10.1002/bip.360221208.
35. He L, Mu C, Shi J, Zhang Q, Shi B, Lin W. Modification of collagen with a natural cross-linker, procyanidin. Int J Biol Macromol. 2011;48(2):354–9. https://doi.org/10.1016/j.ijbiomac.2010.12.012.
36. Covington AD. Tanning chemistry: the science of leather. Cambridge: Royal Society of Chemistry; 2011.
37. Bella J, Brodsky B, Berman HM. Hydration structure of a collagen peptide. Structure. 1995;3(9):893–906. https://doi.org/10.1016/S0969-2126(01)00224-6.
38. Miles CA, Avery NC, Rodin VV, Bailey AJ. The increase in denaturation temperature following cross-linking of collagen is caused by dehydration of the fibres. J Mol Biol. 2005;346(2):551–6. https://doi.org/10.1016/j.jmb.2004.12.001.
39. Bacardit A, Baquero G, Sorolla S, Ollé L. Evaluation of a new sustainable continuous system for processing bovine leather. J Clean Prod. 2015;101:197–204. https://doi.org/10.1016/j.jclepro.2015.04.012.

Publisher's Note